

Suppression of charge order, disappearance of antiferromagnetism, and emergence of ferromagnetism in $\text{Nd}_{0.5}\text{Ca}_{0.5}\text{MnO}_3$ nanoparticles

S. S. Rao,¹ S. Tripathi,² D. Pandey,² and S. V. Bhat^{1,*}¹*Department of Physics, Indian Institute of Science, Bangalore 560012, India*²*School of Materials Science and Technology, Institute of Technology, Banaras Hindu University, Varanasi-221005, India*

(Received 10 July 2006; revised manuscript received 18 August 2006; published 20 October 2006)

$\text{Nd}_{0.5}\text{Ca}_{0.5}\text{MnO}_3$ nanoparticles (average diameter ~ 20 and 40 nm) are synthesized by the polymeric precursor sol-gel method and characterized by various physico-chemical techniques. Quite strikingly, in the 20 nm particles, the charge-ordered (CO) and the antiferromagnetic phases observed in the bulk below 250 K and 160 K, respectively, are completely absent. Instead, a ferromagnetic (FM) transition is observed at 95 K followed by an insulator-to-metal transition at 75 K. The 40 nm particles show a residual CO phase but a transition to the FM state also occurs, at a slightly higher temperature of 110 K.

DOI: 10.1103/PhysRevB.74.144416

PACS number(s): 75.50.Tt, 76.30.-v

I. INTRODUCTION

Nanosized materials, such as nanoparticles, nanowires, nanotubes, and nanocomposites are currently the focus of intense investigations due both to the physics they involve and to their potential for revolutionary technological applications. The applications are expected to be in a wide variety of diverse areas, such as logic circuits, magneto-electronic devices, magnetic data storage, medicine, and biotechnology.¹⁻³ The phenomena and properties behind these applications are unique to nanodimensions, such as quantum confinement effects and enhanced surface to volume ratio. Perovskite manganites having the general formula $R_{1-x}A_x\text{MnO}_3$ (R =rare earth ion, A =alkaline earth ion) exhibit unusual magnetic and electronic properties like colossal magnetoresistance (CMR), charge ordering, orbital ordering, and phase separation due to the strong correlation among spin, electron, and orbital degrees of freedom. The properties of these systems are highly sensitive to the composition, temperature, electric, and magnetic fields.⁴⁻⁶ Further, the transition temperatures T_c from the semiconducting, paramagnetic state to the metallic ferromagnetic state in the CMR compounds are found to either increase or decrease when the material is prepared in nanodimensions.⁷⁻¹⁰ Once the mechanisms of the change in the T_c caused by size reduction are understood, the latter can also be used as an effective way of tuning the properties of these materials. More dramatic are the changes in the properties of CO manganites, where we have recently shown¹¹ that a complete crossover from antiferromagnetic to ferromagnetic phase occurs in nanowires of $\text{Pr}_{0.5}\text{Ca}_{0.5}\text{MnO}_3$ compared to its bulk form, also associated with a weakening of the charge order. In this work, we extend the study to nanoparticles, of $\text{Nd}_{0.5}\text{Ca}_{0.5}\text{MnO}_3$ (NCMO), which is a robust charge-ordering manganite with the charge-ordering temperature $T_{\text{CO}} = 250$ K and the anti-ferromagnetic transition temperature $T_N = 160$ K.⁶ We demonstrate that the CO state can be completely suppressed when the size of the particles is sufficiently small, in addition to the disappearance of the antiferromagnetic phase and the occurrence of the ferromagnetic phase.

II. EXPERIMENTAL

Nanoparticles of NCMO were prepared by the polymeric precursor sol-gel method, also known as the Pechini

method.¹²⁻¹⁴ Though in the original method, dissolution of precursors of cations in an aqueous citric acid solution was used and ethylene glycol was used as a promoter of citrate polymerization, it has been shown to work in the absence of citric acid as well^{7,14} and we have used the latter procedure. In this technique, the polymerized ethylene glycol assists in forming a close network of cations from the precursor solution and helps the reaction enabling the phase formation at low temperatures. The gel forms a resin and the high viscosity of the resin prevents different cations from segregating and ensures a high level of homogeneity. In our preparation, nitrates of neodymium, calcium, and manganese were used as precursors and were dissolved in their stoichiometric ratio in triple-distilled water. An equal amount of ethylene glycol was added with continuous stirring. The solution was heated and the water evaporated on a hot plate whose temperature was increased gradually to 180°C until a thick sol was formed. The sol, in turn, was heated in a furnace at 250°C for about 6 h until a porous material was obtained as a result of complete removal of water molecules. This was further calcined at 600°C and crystalline nanoparticles of NCMO of an average size ~ 20 nm (see below) were obtained. We designated this sample as NCMO-20. A part of this sample was further heated at 900°C for another 6 h to obtain a sample with increased grain size (~ 40 nm). This sample will be called NCMO-40 in the following. For comparison purposes, a NCMO bulk sample was also prepared, using the method of solid state reaction and is labeled NCMO-bulk.

The two samples of NCMO nanoparticles were characterized by various techniques such as x-ray diffraction (XRD), transmission electron microscopy (TEM), energy dispersive x-ray analysis (EDAX), and SQUID magnetometry. The x-ray diffraction patterns, recorded at room temperature [Fig. 1(a)] using a Philips Expert Pro diffractometer and at 12 K [Fig. 1(b)] using a Rigaku 18 kW rotating anode high resolution diffractometer equipped with a closed-cycle refrigeration unit, scanning 2θ in the range 10° – 100° at the rate of $0.01^\circ/10$ s show that the nanoparticles have retained the bulk orthorhombic structure. Elemental composition analysis is done by EDAX and is further checked by inductively coupled plasma atomic-emission spectroscopy. Iodometric titration was used to determine the oxygen percentage. The obtained composition is $\text{Nd}_{0.498}\text{Ca}_{0.491}\text{Mn}_{0.99}\text{O}_{2.98}$. TEM was

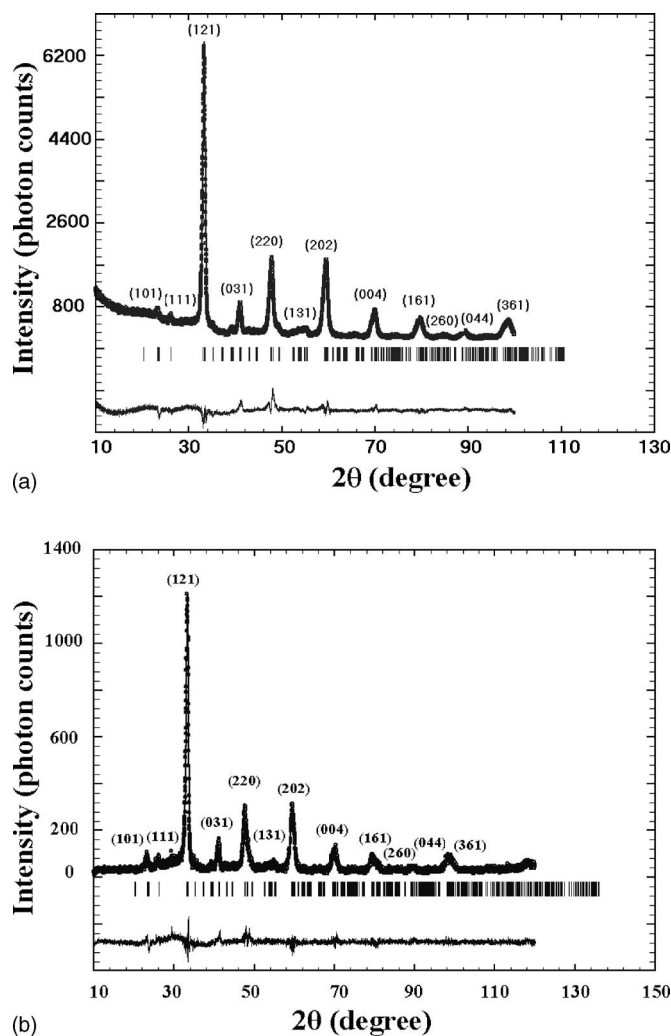


FIG. 1. The observed (dots) and Rietveld fitted (continuous lines) XRD patterns of NCMO-20 nanoparticles at room temperature (a) ($R_w=8\%$) and at 12 K (b) ($R_w=5.4\%$).

used to measure the particle size, size distribution, and the material crystallinity. Magnetization measurements were carried out, using SQUID magnetometry at 500 G on all three samples, viz., NCMO-20, NCMO-40, and NCMO-bulk, in the temperature range 10–300 K. Hysteresis behavior of the magnetization was also studied using the SQUID magnetometer at three different temperatures (10, 75, and 175 K) for NCMO-20. The temperature dependence of the resistance of pellets of NCMO-20 and NCMO-bulk was studied using a four-probe setup.

III. RESULTS AND DISCUSSION

Figure 1 shows the x-ray diffraction patterns of NCMO-20 nanoparticles recorded at RT (a) and 12 K (b). The crystallite size is estimated to be ~ 15 nm from the width of the peaks using the Scherrer formula. The size was also estimated from the TEM picture shown in Fig. 2(a), which shows the presence of single isolated nanoparticles, of size ~ 20 nm, in addition to the aggregated ones. In order to obtain the structural parameters, the diffraction data in Fig. 1

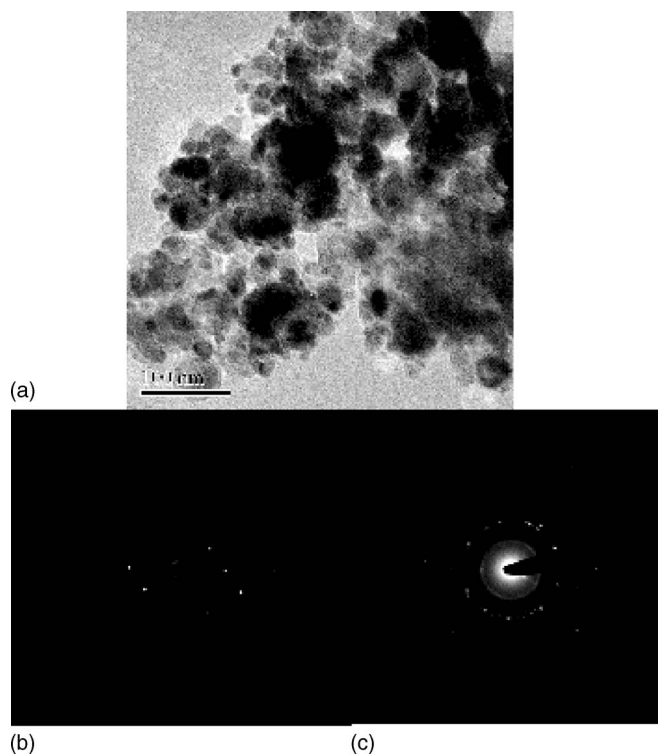


FIG. 2. (a) A TEM micrograph of NCMO-20 nanoparticles: the scale bar corresponds to 100 nm in length. (b) and (c): the SAED patterns in different regions showing diffraction spots (b) indicating single crystalline nature and rings (c) indicating polycrystalline behavior.

were analyzed, using the Rietveld powder diffraction profile fitting technique. NCMO-20 crystallizes in the orthorhombic space group $Pnma$ with the unit cell parameters $a=5.4180$ Å, $b=7.5809$ Å, and $c=5.3798$ Å. (unit cell volume $V=220.97$ Å³). The corresponding bulk values are $a=5.4037$ Å, $b=7.5949$ Å, and $c=5.3814$ Å (Ref. 15) ($V=220.855$ Å³). One could fit the 12 K pattern as well with the same space group ($Pnma$) with $a=5.4171$ Å, $b=7.5428$ Å, $c=5.3747$ Å, and $V=219.61$ Å³. The selective area electron diffraction (SAED) pattern (Fig. 2) shows that some of the nanoparticles are single crystalline, as seen by the sharp spots [Fig. 2(b)] and some are polycrystalline, giving rise to the diffraction rings [Fig. 2(c)].

Figure 3 shows the temperature dependence of magnetization of NCMO-20 and NCMO-40 nanoparticles compared with their bulk counterpart NCMO-bulk in the same figure. It is well known^{6,16} that the CO transition is characterized by a peak in the magnetization where the double exchange is suppressed due to the localization of the charge carriers, resulting in a large drop of the susceptibility. The bulk NCMO sample shows this charge ordering peak at 250 K. The antiferromagnetic transition is normally indicated by a much weaker feature in the M vs T dependence and in the case of NCMO bulk sample it is established that $T_N=160$ K⁶ though on the scale of the figure it is not clearly visible. The AF transition was also confirmed by the disappearance of the EPR signal below 160 K.¹⁷ The CO peak is seen to have decreased in intensity for the NCMO-40 (size ~ 40 nm)

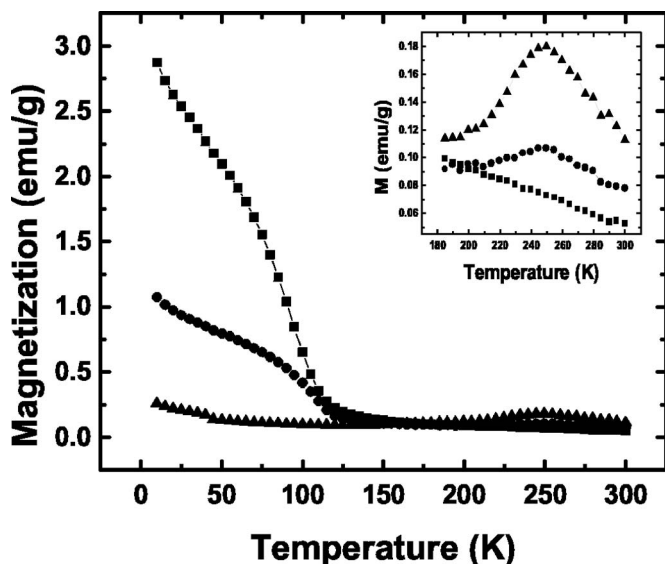


FIG. 3. The magnetization versus temperature for NCMO-20 (squares), NCMO-40 (circles), and NCMO-bulk (triangles). The inset shows the results in an expanded temperature scale in the range 180–300 K. The weakening of the CO peak in NCMO-40 and the disappearance of the same in NCMO-20 are clearly seen. The feature at ~160 K in the bulk NCMO, indicating the AF transition is too weak to be seen on this scale.

sample and in the case of NCMO-20 sample (size ~20 nm) it is entirely absent (inset). This conclusion is also supported by the XRD pattern at 12 K, shown in Fig. 1(b), where the splitting of the peaks indicative of superlattice reflections due to charge ordering is seen to be absent. In addition, while the bulk NCMO undergoes an AF transition at 160 K, both in NCMO-20 and NCMO-40 the AF phase is absent. Instead, they show increases in magnetizations below about 125 K indicative of ferromagnetic transitions. From the minima in the temperature derivatives dM/dT of magnetizations the two transition temperatures were determined to be 95 and 110 K, respectively.

The occurrence of ferromagnetism is also confirmed by the observation of hysteresis in the M vs H behavior as shown in Fig. 4 for 10 K contrasted with the behavior for $T > T_C$ (175 K). We further note that $M(H)$ does not saturate till the highest fields [5 T, inset (a) to Fig. 4] we have used. This behavior is reminiscent of superparamagnetism. However, there is one essential difference: the latter are ferromagnetic in bulk while the present samples are not. We have estimated the FM fraction, using the value of magnetization at 10 K at the highest field available to us (i.e., 5 T) and it comes to around 1.04 Bohr magnetons (μ_B) per formula unit, compared to the expected value of $3.5\mu_B$ (i.e., about 30 %) for Mn only ordering. Though the value is an underestimate since the value of magnetization used for the estimate is much less than its saturation value, one cannot rule out the possibility that the whole sample may not be ferromagnetic, especially since the contribution of the disordered (and therefore nonmagnetic) surface layers is quite significant in the nanoparticles. However, we can certainly conclude that most of the magnetization is from the interior of the nanoparticles with suppressed Jahn-Teller distortions since the surface Mn

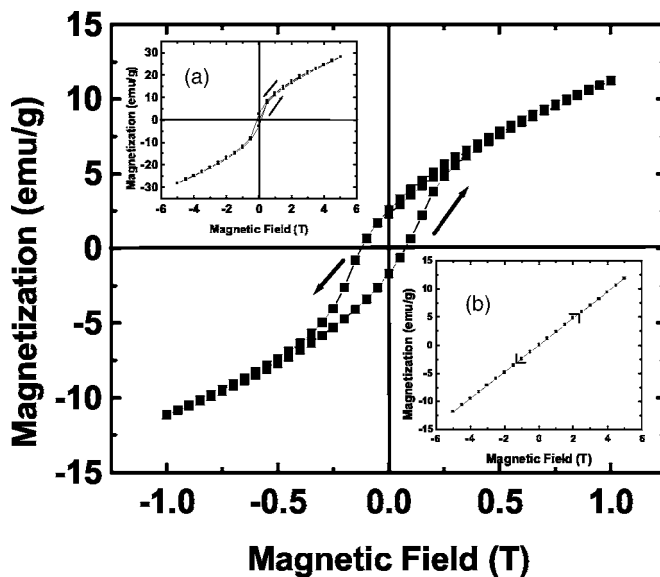


FIG. 4. The M vs H plot for NCMO-20 at 10 K (main panel) and at 175 K [inset (b)]. Hysteresis indicative of ferromagnetism is clearly seen. Inset (a) shows the absence of saturation until 5 T.

ions constitute only 1–5 % of the total Mn in the 20 and 40 nm particles. It is known that the insulating charge-ordering state can be “melted” by the application of either a magnetic field or an electric field and also by irradiation with photons or by doping with certain ions.^{6,18} However, in the present work we find that without using any external perturbations, just by reducing the particle size to a few nanometers, the insulating, charge-ordered state is suppressed and the AF phase is replaced by an FM phase. Similar results have been observed by us in the case of $\text{Pr}_{0.57}\text{Ca}_{0.41}\text{Ba}_{0.02}\text{MnO}_3$ ¹⁹ as well. In Fig. 5 we present the hysteresis observed at 75 K, close to the ferromagnetic T_C . It

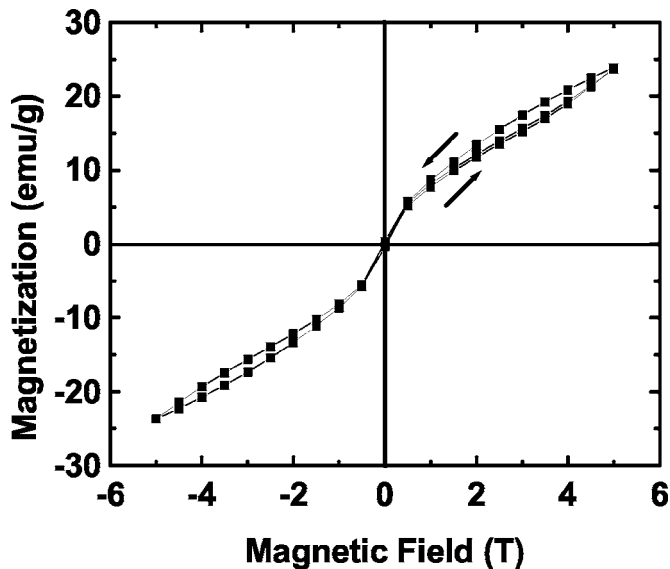


FIG. 5. The M vs H plot for NCMO-20 at 75 K. The nature of the hysteresis is indicative of metamagnetic behavior, also observed in systems which show magnetic field induced melting of the CO state (Refs. 20 and 21).

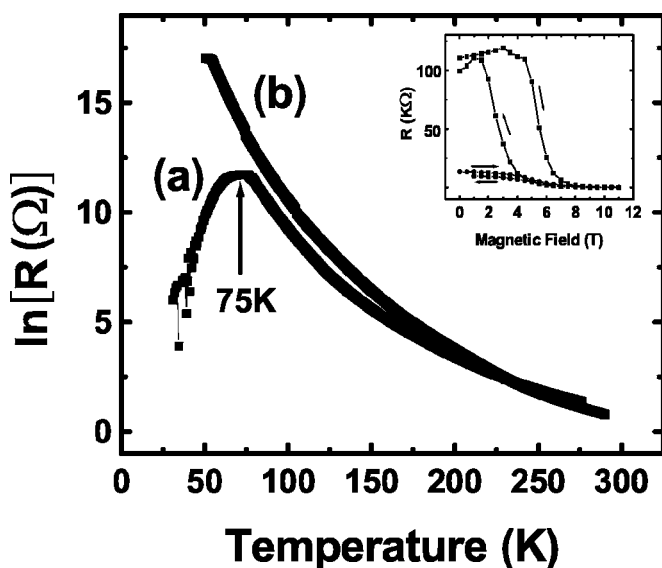


FIG. 6. Temperature dependence of the resistance of NCMO-20 (a) nanoparticles compared with that of (b) bulk. The insulator-to-metal transition at 75 K in the nanoparticles is clearly seen. The inset shows the resistance behavior of NCMO-20 for forward and reverse scans of the magnetic field at 75 K (squares) and 100 K (circles). The large hysteresis observed at 75 K confirms the ferromagnetic nature of the nanoparticles.

is seen that at this temperature M vs H shows metamagnetic behavior similar to that observed in systems showing magnetic-field induced melting of the CO state.^{20,21}

Contactless conductivity and four-probe resistivity measurements were done to study the electrical transport property of the material in the ferromagnetic phase. From contactless conductivity method an enhancement in the conductivity of the NCMO-20 nanoparticles was observed. For the four-probe resistivity measurements, the required pellets were prepared under a pressure of 150 psi and the pellets were then sintered at 300 °C for 2 h, the parameters ensuring that particle size did not increase. Silver paste was used to make contacts to the electrodes. As shown in Fig. 6, a peak in the temperature dependence of resistance indicative of a metal insulator transition is seen at 75 K. A large resistive hysteresis as a function of the magnetic field at 75 K (shown in the inset) is also observed, confirming the FM phase at this temperature. A high CMR ($\sim 99.8\%$) was observed at 75 K at a field of 11 T. The details of these measurements will be published elsewhere.

Now we discuss a possible explanation of this interesting phenomenon. We note that until now no complete disappearance of the CO state has been observed in any nanomanganite. However, some reports on CMR nanomanganites have appeared⁷ recently, providing evidence for an increase in the T_C compared to that in the bulk. This observation is explained in terms of a change in the cell parameters, reduction in the unit cell volume, and consequent increase in the symmetry. In the present case though, the unit cell volume at RT in the nanoparticles is actually (though only marginally) larger than that in the bulk. Further, the relevant bond angles and the bond lengths also did not show any significant changes (157.10° in nano vs 157.05° in bulk; 1.95 \AA in nano

vs 1.948 \AA in bulk). Moreover, comparing the structural parameters of the nanoparticles at RT with those at low temperature, we find that the mean distortion Δ_d in the MnO_6 octahedra defined by $\Delta_d = 1/6 \sum_{i=1}^6 [(d_i - \langle d \rangle) / \langle d \rangle]^2$ where d is the Mn-O bond length (Ref. 15), is found to be 1.658×10^{-5} at RT and 3.297×10^{-5} at 12 K. Thus the mean orthorhombic distortion has actually increased by a factor of 2 at 12 K compared to that at RT . Therefore, it is quite unlikely that the mechanism proposed earlier⁷ in terms of an increase in the symmetry leading to an increase in the T_C of CMR manganites in nanodimensions is operative here. Indeed it is conceivable that a fundamentally different explanation connected with the fine balance between the competing interactions, namely, the one that leads to the CO state and the other that leads to the FM state needs to be sought for the present observation.

In an effort to understand the mechanism of the suppression of the CO and AFM phases and the appearance of the FM phase in nanomanganites it is relevant to note that for $T > T_{CO}$, in the bulk paramagnetic insulating state, ferromagnetic correlations are already present^{22,6} originating in the thermally activated hopping of the e_g electrons. These ferromagnetic spin fluctuations change to antiferromagnetic fluctuations at T_{CO} and subsequently lead to the AFM-ordered state at T_N . Therefore, if the CO transition is suppressed through some mechanism, the already present FM correlations could lead to an FM ordered state at a lower temperature. We believe that in the nanoparticles of NCMO the mechanism of the suppression of the CO transition is provided by the surface disorder. This can happen in either or both of the two following processes: it is understood that the charge ordering in the half-doped manganites is achieved via a sequence of incommensurate configurations^{23,24} associated with the movement of extended charge-ordering planar defects also known as discommensurations. In nanoparticles, these discommensurations could get pinned at the surface hindering their movement and thus preventing the establishment of long-range charge order. Alternatively, the disorder present in the surface extending to a few layers into the interior of the nanoparticles may prevent the formation of the long-range charge ordered state. However, the ferromagnetic order can still occur due to the short-range nature of the exchange interactions since the FM fluctuations are already present at higher temperatures. While these are possibilities, we note that much more work needs to be done along these ideas; however, that is beyond the scope of the present work.

IV. CONCLUSION

In summary, NCMO nanoparticles were prepared by polymeric precursor sol-gel method. The particles were characterized by different techniques like XRD, TEM, iodometry, ICPAES, EDAX, and SQUID magnetometry. It is shown that the charge-ordered and the antiferromagnetic phases observed in the bulk disappear in the nanoparticles making way for an “emergent” ferromagnetic metallic phase.

ACKNOWLEDGMENTS

S.S.R. would like to thank CSIR, Government of India for financial support.

*Corresponding author. Email address:

svbhat@physics.iisc.ernet.in

- ¹P. R. Bandaru, C. Daraio, S. Jin, and A. M. Rao, *Nat. Mater.* **4**, 663 (2005).
- ²L. Krusin-Elbaum, D. M. Newns, H. Zeng, V. Derycke, J. Z. Sun, and R. Sandstrom, *Nature (London)* **437**, 672 (2004).
- ³O. V. Salata, *J. Nanobiotechnology* **2**, 3 (2004).
- ⁴*Colossal Magnetoresistance, Charge Ordering and Related Properties*, edited by C. N. R. Rao and B. Raveau (World Scientific, Singapore, 1998).
- ⁵*Colossal Magnetoresistive Oxides*, edited by Y. Tokura (Gordon and Breach Science Publishers, New York, 2000).
- ⁶F. Millange, S. de Brion, and G. Chouteau, *Phys. Rev. B* **62**, 5619 (2000).
- ⁷K. S. Shankar, S. Kar, G. N. Subbanna, and A. K. Raychaudhuri, *Solid State Commun.* **129**, 479 (2004).
- ⁸A. Dutta, N. Gayathri, and R. Ranganathan, *Phys. Rev. B* **68**, 054432 (2003).
- ⁹G. Venkataiah, D. C. Krishna, M. Vithal, S. S. Rao, S. V. Bhat, V. Prasad, S. V. Subramanyam, and P. Venugopal Reddy, *Physica B* **357**, 377 (2005).
- ¹⁰M. A. Lopez-Quintela, L. E. Hueso, J. Rivas, and F. Rivadulla, *Nanotechnology* **14**, 212 (2003).
- ¹¹S. S. Rao, K. N. Anuradha, S. Sarangi, and S. V. Bhat, *Appl. Phys. Lett.* **87**, 182503 (2005).
- ¹²M. A. L. Nobre, E. Longo, E. R. Leite, and J. A. Varela, *Mater. Lett.* **28**, 215 (1996).
- ¹³E. C. Paris, E. R. Leite, E. Longo, and J. A. Varela, *Mater. Lett.* **37**, 1 (1998).
- ¹⁴Xi Li, H. Zhang, F. Chi, S. Li, B. Xu, and M. Zhao, *Mater. Sci. Eng., B* **18**, 209 (1993).
- ¹⁵O. Richard, W. Schuddinck, G. Van Tendeloo, F. Millange, M. Hervieu, V. Caignaert, and B. Raveau, *Acta Crystallogr., Sect. A: Found. Crystallogr.* **55**, 704 (1999).
- ¹⁶D. Niebieskikwiat and M. B. Salamon, *Phys. Rev. B* **72**, 174422 (2005).
- ¹⁷J. P. Joshi, R. Gupta, A. K. Sood, S. V. Bhat, A. R. Raju, and C. N. R. Rao, *Phys. Rev. B* **65**, 024410 (2001).
- ¹⁸C. N. R. Rao, A. R. Raju, V. Ponnambalam, S. Parashar, and N. Kumar, *Phys. Rev. B* **61**, 594 (2000).
- ¹⁹K. N. Anuradha, S. S. Rao, and S. V. Bhat, *J. Nanosci. Nanotechnol.* (to be published).
- ²⁰Y. Tomioka, A. Asamitsu, Y. Moritomo, H. Kuwahara, and Y. Tokura, *Phys. Rev. Lett.* **74**, 5108 (1995).
- ²¹Y. Tokura, H. Kuwahara, Y. Moritomo, Y. Tomioka, and A. Asamitsu, *Phys. Rev. Lett.* **76**, 3184 (1996).
- ²²Wei Bao, J. D. Axe, C. H. Chen, and S-W. Cheong, *Phys. Rev. Lett.* **78**, 543 (1997).
- ²³P. G. Radaelli, D. E. Cox, M. Marezio, and S-W. Cheong, *Phys. Rev. B* **55**, 3015 (1997).
- ²⁴Z. Jirak, F. Damay, M. Hervieu, C. Martin, B. Raveau, G. Andre, and F. Bouree, *Phys. Rev. B* **61**, 1181 (2000).